Journal of Optoelectronics and Advanced Materials Vol. 2,. No. 5, 2000, p. 704-712

Section 10: Special topics *INVITED*

STRUCTURE ANISOTROPY OF HIGH-TEMPERATURE SUPERCONDUCTORS: RESISTANCE PEAK EFFECT

C. Buzea[a,b], T. Yamashita[b,c]

[a] Research Institute of Electrical Communication, Tohoku University, Sendai 980-8577, Japan
[b] New Industry Creation Hatchery Center, Tohoku University, Sendai 980-8579, Japan
[c] CREST Japan Science and Technology Corporation (JST)

An anomalous resistive peak has been observed for various low- and high-temperature superconductors. Due to diversity in sample configuration and material properties, it is unclear if the various peak observations are related to each other and in which way. Here we present theoretical calculations based on electrical circuits that demonstrate the resistive peak effect can be entirely accounted by material anisotropy - which generates an apparent critical temperature (T_c) anisotropy. The experiments performed on $La_{2-x}Sr_xCuO_4$ films fit well the proposed theory of T_c anisotropy.

Keywords: Low-Tc superconductors, High-Tc superconductors, Resistance peak, Critical temperature, Anisotropy

1. Introduction

In the last two decades an anomalous Resistance Peak Effect (RPE) has been observed when measuring the resistance of various superconductors. The RPE can be described as an increase in the resistance above the normal-state value, R_n, foregoing the transition from superconducting to normal state.

This paper is organised as follows. Section 2 contains a short review of the experiments which show the resistance peak in various superconductors. Sections 3 presents a theoretical approach for the resistance peak effect based on a simple electrical circuit model. The results of the theoretical model states the necessity of critical temperature anisotropy for the appearance of the RPE. In Section 4 we propose different explanations for the critical temperature anisotropy, which include critical current anisotropy, coherence lengths anisotropy, or interplay between Kosterlitz-Thouless temperature and Josephson coupling energy. Section 5 shows experiments performed on $La_{1.85}Sr_{0.15}CuO_4$ (LSCO) thin films which demonstrate the validity of our theoretical explanation. Section 6 concludes the paper.

2. Materials which exhibit resistance peak

The RPE has been observed in a wide variety of systems: quasi-two-dimensional superconductors - $TaSe_3$ [1]; artificially layered superconductors - $Nb_3(GeSi)$ [2], Au/Ge [3]; inhomogeneous low-Tc superconductors - Cu-Zr [4], (NbV)N, NbN, VN, (NbTi)N [5]; Al thin films and mesoscopic wires [6]; intrinsic layered superconductors - $L_{2-x}Ce_xCuO_4$ (L=Pr, Nd, Sm) and $La_{2-x}Sr_xCuO_4$ [7], [8], $YBa_2Cu_3O_7$ [9], and $Bi_2Sr_2CaCu_2O_8$ [10].

These systems range from one-dimensional to bulk samples, low-T_c superconductors (LTSC) to high-T_c superconductors (HTSC), single component to multicomponent systems, polycrystalline materials to single crystals, artificially layered to intrinsic layered superconductors.

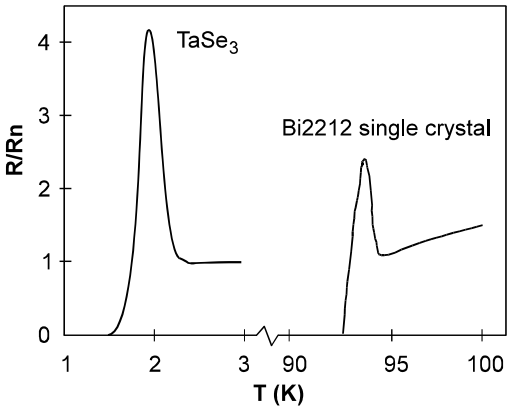

Fig. 1. Resistance peak of $TaSe_3$ (after ref. [1]) and Bi2212 (after ref. [10]).

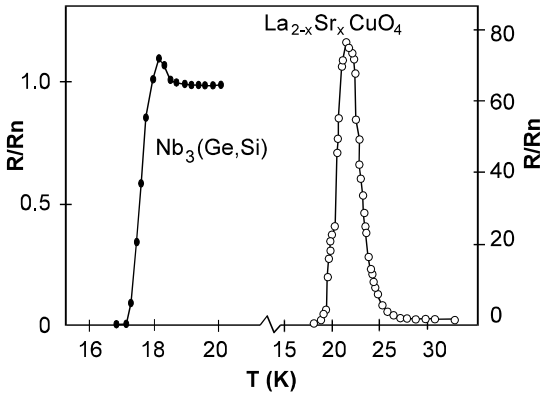

Fig. 2. Resistance peak for Nb3(Ge,Si) (after ref. [2]) and $La_{2-x}Sr_xCuO_4$ (after ref. [8]).

The peaks are similar in magnitude or shapes for different types of superconductors. Similar features occur for LTSC and HTSC. For example in Fig. 1 are given the peaks exhibited by a $TaSe_3$ [1] and Bi2212 sample [10]. The magnitude R_p and width ΔT of the peak for both materials have similar values, namely R_p=4 and 2.5, and ΔT=1K and 2K, respectively.

However, the peak magnitude can attain up to 80 times the resistance in the normal state or be very small (see Fig. 2). Also, the width of the peak can be very large, of up to 15 K. The peak can be different for samples made from the same material, as shown in Fig. 3.

The superconductors were measured using in-plane strip contacts or four-point contact configuration, as depicted in Fig. 4. Due to the diversity in sample configuration and material properties, it is unclear if the various peak observations are related to each other and in which way. Despite the fact that several explanations have been proposed in order to explained the anomaly, its physical origin is still not understood and the question whether it has a common origin is still open.

3. Theory - critical temperature anisotropy

We noticed that all the materials which exhibit the RPE are either layered (intrinsic or artificially), granular or inhomogeneous. This means that the measured resistance R for the case of out-of-plane four point contact configurations will be a mathematical expression containing the in-plane and out-of-plane resistance (for layered materials) or the resistances of different grains or multi-phases (for inhomogeneous materials). In the case of in-line stripe contacts, a small misalignment will generate the inclusion of both in-plane and out-of-plane resistaces in the expression of R for layered materials, as well as the resistances of different grains or multi-phases for inhomogeneous materials.

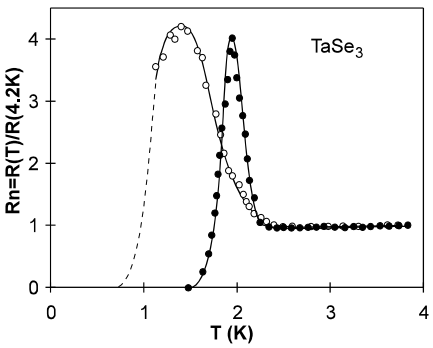

Fig. 3. R versus T for two $TaSe_3$ samples [1].

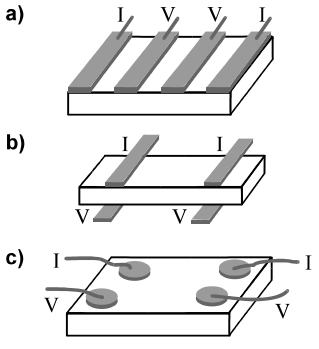

Fig. 4. Contact configurations used in measuring RPE.

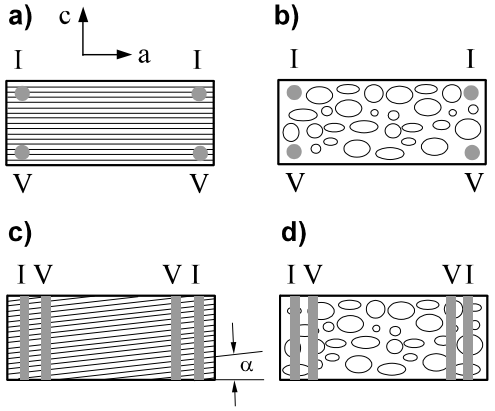

Fig. 5. Structural details of the layers or grains for layered or inhomogeneous superconductors measured with in-line stripe contacts and out-of-plane four point contacts.

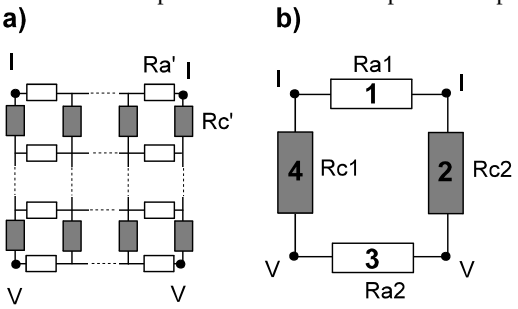

Fig. 6. a) Equivalent electrical circuit, b) simplified equivalent electrical circuit.

The only possible cause which would lead to a resistance peak appearance is the existence of two different critical temperatures for in-plane and out-of-plane resistances or for different grains (see Fig. 5).

In the case of inhomogeneous materials, the RPE can be determined by using the percolation theory.

A more interesting case is the one of layered superconductors, which we will discuss in the following. The contact configuration from Fig. 5.a) can be approximated by the circuit from Fig. 6.a), with the number of meshes corresponding to the number of layers along c-axis and to the number of unit cells along a-axis. The use of less meshes does not change appreciably the results of this approximation. Therefore, we will consider the simplest case, with four resistors, as shown in Fig. 6.b). The measured resistance of the circuit with the contact configuration from Fig. 6.b) is

$$R = \frac{R_{a1}R_{a2}}{R_{a1} + R_{a2} + R_{c1} + R_{c2}} = \frac{R_a^2}{2\left(R_a + R_c\right)} = \frac{R_a}{2} \cdot \frac{1}{1 + \frac{R_c}{R_a}} \tag{1}$$

when $R_{a1}=R_{a2}=R_a$, and $R_{c1}=R_{c2}=R_c$.

We have three different cases:

a) $T_c^a=T_c^c$; obviously, if the critical temperature of Ra and Rc are identical, the measured resistance R will have a normal transition into superconductive state.

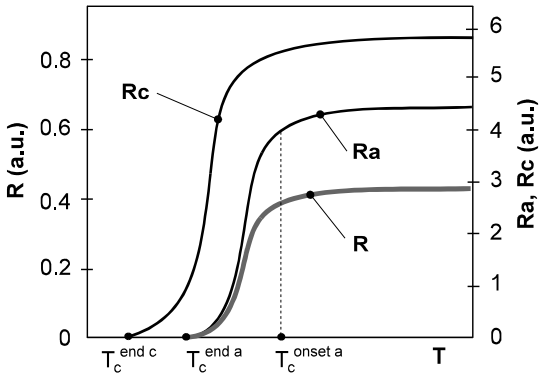

Fig. 7. R, Ra and Rc for the case when T_c along a-axis is higher than T_c along c-axis.

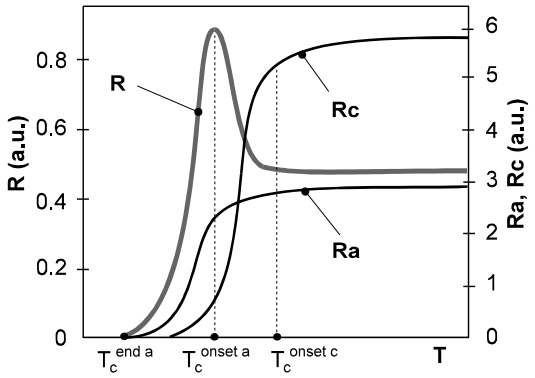

Fig. 8. R, Ra and Rc for the case when T_c along c-axis is higher than T_c along a-axis.

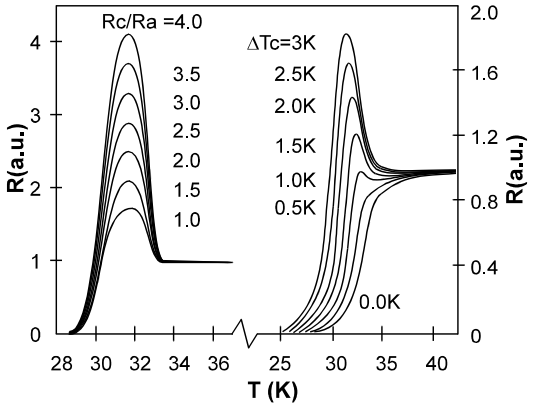

Fig. 9. Resistance peak for different values of r and ΔT_c.

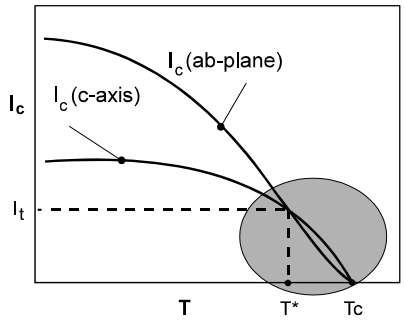

Fig. 10. Critical current versus T.

b) $T_c^a > T_c^c$; in this case, in Eq. (1), the denominator will decrease slower than the nominator due to the presence of Rc, whose transition is delayed compared to Ra. The transition of R is depicted in Fig. 7.

c) $T_c^a < T_c^c$; the denominator of Eq. (1) will decrease faster than the nominator, leading to the appearance of the peak, as shown in Fig. 8. The temperature for which R will start an upward curvature is the temperature for which the resistance along c-axis starts to decrease, $T_c^{onset\ c}$. The peak maxima Rp is attained for approximately the same temperature for which the Ra starts to decrease $T_c^{onset\ a}$. Finally, R will pass in superconductive state when Ra is zero, at $T_c^{end\ a}$.

Therefore, the peak appears only when the critical temperature along c-axis is higher than the critical temperature along a-axis. More exactly, when T_c perpendicular to the layers is higher than T_c parallel to the layers (CuO planes in high-T_c superconductors).

We found two parameters of variation for the resistance peak effect: the ratio r=Rc/Ra, and the difference in the critical temperature between c- and a-axis, ΔT_c. In Fig. 9 (left side) we plotted R versus T for different values of Rc/Ra considering ΔT_c =3K. One notices that when Rc is much larger than Ra, the peak maxima Rp will be higher. The peak also exists for Ra=Rc. In Fig. 9 (right side) we plotted R versus T for different values of ΔT_c considering Rc/Ra fixed at 2. For ΔT_c=0 K and 0.5 K the peak cannot be observed in the R-T transition. The peak starts to develop for ΔT_c=1K, increasing in magnitude with larger ΔT_c.

4. Critical temperature anisotropy - possible causes

4.1. Critical current anisotropy

We showed above that T_c along c-axis should be higher than T_c along a-axis in order to have a resistive peak. Is this critical temperature anisotropy real or only apparent? One possible scenario is related to different transport mechanisms along and perpendicular to the CuO planes. It is well known that the critical current along ab-plane (CuO layers) can be described by a thermally activated flux creep model [11]

$$I_c(ab-plane) = I_c(0)\cdot\left[1-(T/T_c)^2\right]^m \tag{2}$$

where m is a scaling parameter. The electrical transport along c-axis can be described by the Ambegaokar-Baratoff relation for tunnel junctions [12]

$$I_c(c-axis) = \frac{\pi\Delta}{2eR_n}\tanh\frac{\Delta}{2K_BT};\ with\ \Delta = \Delta(0)\cdot\left[1-(T/T_c)^4\right] \tag{3}$$

where R_n is the junction resistance in the normal state and Δ is the energy gap. In Fig. 10 we plotted together the critical current along ab-plane and c-axis given by Eqs. (2) and (3). At low T, the supercurrent flows more easy in the CuO planes than perpendicular to these planes. One notices that between zero Kelvin and a temperature T*, the critical current along ab-plane is larger than critical current along c-axis. The situation reverses between T* and T_c.

If the applied current I_{app} is smaller than the threshold value of the current I_t (see Fig. 11) for which the critical current along ab-plane is equal to the critical current along c-axis (at T*), then we will have the following picture. The resistance along c-axis will become zero when the value of the critical current along c-axis is higher than the value of the applied current, I_{app}, namely at a temperature smaller than the critical temperature of the material, T_c^c, as can be seen in Fig. 11. At this temperature the critical current along ab-plane is still smaller than the value of the applied current, I_{app}. Therefore, for the fixed value of the applied current I_{app}, apparently, along ab-plane the superconductivity is not achieved yet at temperatures between T_c and T_c^c. Decreasing more the temperature below, at a value equal to T_c^{ab} the current along ab-plane will exceed the value of the applied current I_{app}, and finally, the resistance along ab-plane will become zero too (Fig. 11).

For the case of $La_{2-x}Sr_xCuO_4$, in Fig. 12.a) we plotted the critical currents dependence on temperature given by Eqs. (2) and (3). We considered a critical temperature T_c = 39K, the critical current density along ab-planes of about $10^6 A/cm^2$, a ratio of the critical currents along ab-plane and c-axis of 5, the value of the coefficient m = 3.2, and the energy gap at zero Kelvin $\Delta(0)=K_BT_c$. For an applied current I_{app} = 10 μA we may observe an apparent critical temperature anisotropy, namely the critical temperature along c-axis of about 36K and along ab-plane of about 34K, in agreement with the experimental observations described later in this paper.

The critical temperature anisotropy ΔT_c can vary with the applied current value. The general case is depicted in Fig. 12 b). If I_{app} is situated in regions A or C, a variation of ΔT_c will be observed when modifying I_{app} [1]. If the applied current is varied and the its values are situated in the region B from Fig. 12.b), then ΔT_c will be almost constant for increasing the applied current, therefore no peak variation will be observed with the modifications in the value of the I_{app}. This is the case of high-T_c superconductors, where the peak magnitude remains constant for different values of the applied current.

In conclusion, when measuring the equivalent resistance of the circuit from Fig. 5.a) with the current contacts along ab-plane, we will observe an apparent anisotropy of T_c along ab-plane and c-axis, the value of the anisotropy value being dependent on the value of the applied current I_{app}.

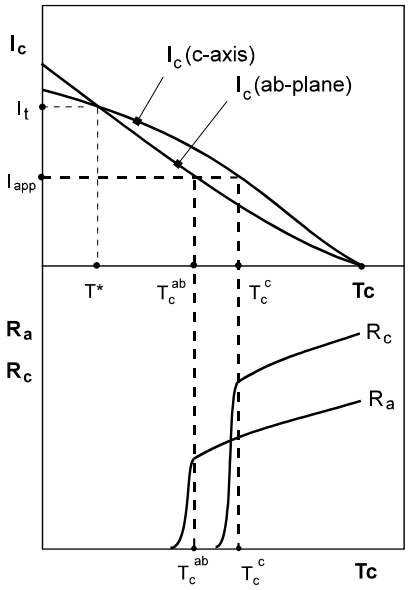

Fig. 11. Resistance and critical current along ab-plane and c-axis versus T near T_c.

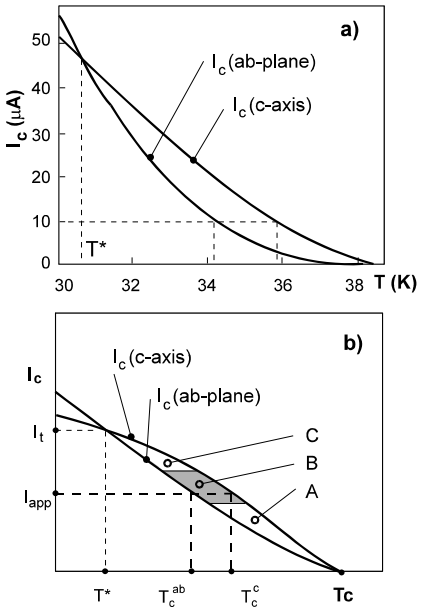

Fig. 12. I_c along ab-plane and c-axis vs. T given by Eqs. (2) and (3), near T_c for a)LaSrCuO sample b) general case.

4.2. Anisotropic coherence lengths

Usually, the coherence lengths values at zero Kelvin of high-temperature superconductors are about $\xi_c(0)$=0.1 nm and $\xi_{ab}(0)$=3 nm [13]. Also, most of cuprates have an intrinsic granularity, i. e. due to compositional modulation the structure is not uniform. Near T_c this fact may play an important role because the coherence length must be smaller than the dimension of intrinsic granularity in order the region to be superconductive. In Fig. 13 we plotted the coherence lengths dependence on temperature for different values of $\xi(0)$ = 0.1, 0.5, 1, 1.5, 2, 2.5, 3, 3.5 nm in three cases, a) T_c=30 K, b) T_c=35 K, and c) T_c=80 K. Indeed, as we can notice in Fig. 13, for a value of 20 nm for the dimension of intrinsic granularity, the coherence length along c-axis becomes smaller than 20 nm just near T_c at 30, 35 and 80 K, respectively. This means that along c-axis superconductivity is achieved at T_c. But this is not the case along ab-plane, due to the fact that ξ_{ab} becomes smaller than 20 nm at lower temperatures. Therefore superconductivity along ab-planes appears at T lower than T_c, leading to an anisotropy in the critical temperature along c-axis and ab-plane of about a) 0.5, b) 0.6 K, and c) 1.3 K, respectively, for the three cases presented.

4.3. Interplay between Kosterlitz-Thouless temperature and Josephson coupling energy

Another probable explanations of RPE is related to thermal fluctuations of vortices and antivortices [14]. T_c anisotropy may be due to the interplay between the Kosterlitz-Thouless (KT) transition temperature, T_{KT}, and Josephson coupling energy. Thermal fluctuations at low temperatures result in the production of vortex-antivortex pairs, called intrinsic vortices, where the flux screening currents of an antivortex flow in a direction opposite to that of a vortex. A vortex and antivortex attract each other; at low T they form bound pairs that dissociate at T_{KT}. In a high anisotropic system, the KT transition plays an important role in the CuO planes, while Josephson coupling is the dominant effect along the c axis. In a T range below and closed to T_c, Ra remains at a finite value (due to thermal fluctuations of free vortices and antivortices), decreasing slowly until T reaches the vortex-unbinding KT transition temperature. On the other hand, due to interlayer Josephson coupling at T_c, Rc decreases by orders of magnitude, the peak appearing due to an abrupt decrease in anisotropy.

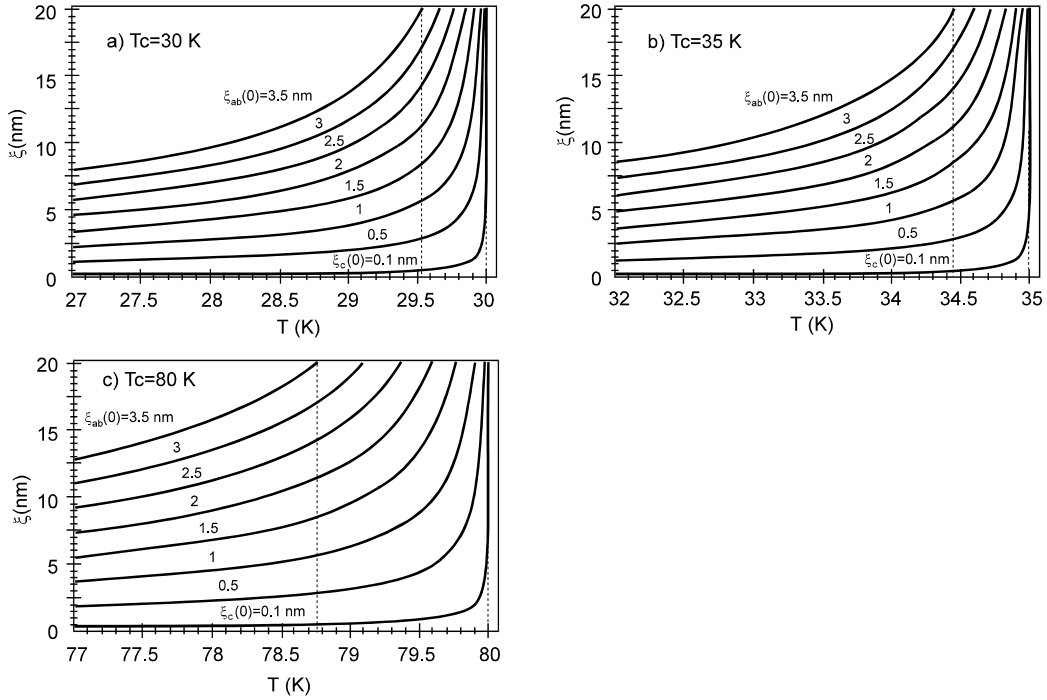

Fig. 13. The coherence length versus T for ξ(0) = 0.1, 0.5, 1, 1.5, 2, 2.5, 3, 3.5 nm in the case of a) T_c=30 K, b) T_c=35 K, c) T_c=80 K.

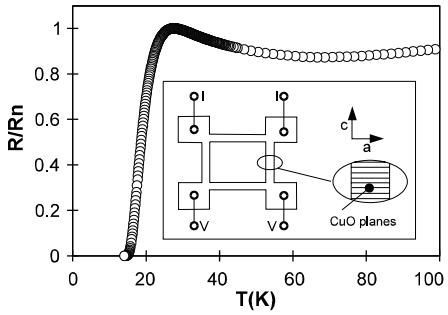

Fig. 14. R versus T of a patterned LSCO sample.

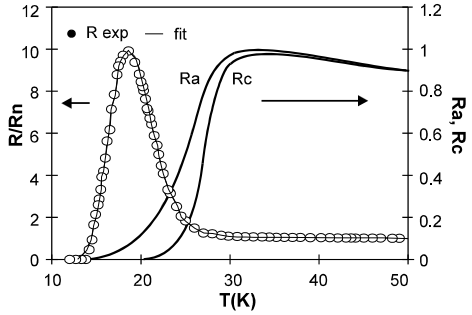

Fig. 15. R fitted by Ra and Rc versus T.

5. Experimental

In order to verify the hypothesis of critical temperature anisotropy along c-and a-axis, we performed resistive measurements on $La_{1.85}Sr_{0.15}CuO_4$(100) films (LSCO). The fabrication procedure is described elsewhere [15]. Transport properties of the films were measured by conventional four probe method. Some of the films were patterned with bridges along c- and a-axis.

Not all the films presented the anomalous resistance peak, even when patterned (see Fig. 14). Other patterned LSCO samples exhibit a very large peak, the peak maxima being ten times higher than the resistance in the normal state, as seen in Fig. 15. The peak was fitted with the values of the Ra and Rc shown on the same plot, with $T_c^{onset\ c}$=34 K, $T_c^{end\ c}$=20 K, $T_c^{onset\ a}$=32.5 K, and $T_c^{end\ a}$=15 K. The fitting ratio r=Rc/Ra =3100 at 50 K.

Due to the small size of bridges compared to the contact portion, the measurement of the resistances along each axis (a or c) had influences from the another axis, making impossible an accurate determination of T_c along each axis. Therefore, as a final demonstration of apparent T_c

anisotropy leading to RPE, we performed a resistive measurements on four separate LSCO samples, we determined T_c for each one, after which the samples were connected in a four-point-type contact configuration, as shown in Fig. 16 inset, and the resistance of this configuration measured.

Samples with Ra1, Rc1 were cut from the same film, with the orientation from Fig. 16 inset, one along a-axis and one along c-axis. The individual resistances of each film are shown in Fig. 16.a). One notices a critical temperature anisotropy, T_c along a-axis being $T_c^{onset\ a}$=34 K, $T_c^{end\ a}$=23 K, and along the c-axis $T_c^{onset\ c}$=36 K, $T_c^{end\ c}$=26 K. Samples Ra2 and Rc2 were also cut from the same film.

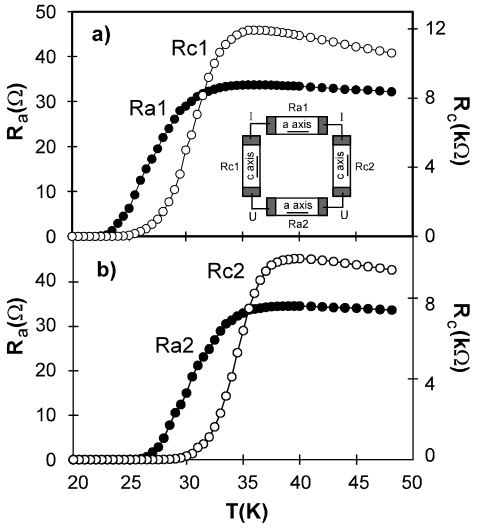

Fig. 16. Ra1, Rc1, Ra2 and Rc2. Inset is the schematic configuration of the four-sample type measurement.

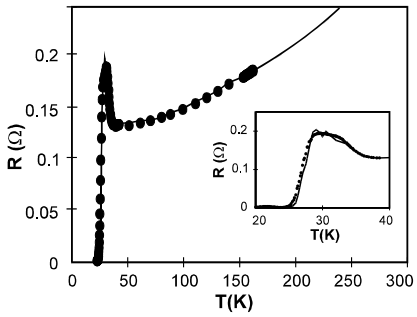

Fig. 17. The measured resistance R versus temperature T for the four - sample configuration.

The temperature dependence of each sample resistance is presented in Fig. 16.b), where a critical temperature anisotropy of more than 3 K can be noticed. T_c along a-axis is: $T_c^{onset\ a}$=35 K, $T_c^{end\ a}$=26 K, and along the c-axis $T_c^{onset\ c}$=38 K, $T_c^{end\ c}$=30 K.

After measuring each samples individually, the samples were connected like in Fig. 16 inset and a four-point-type contact resistive measurement was performed. This configuration exhibits the resistance peak seen in Fig. 17. The experimental data of the peak were fitted by using Eq. (1), where we inserted the experimental values obtained for each resistances, Ra1, Ra2, Ra3, Ra4. In Fig. 17 inset one notices that the fitting is very closed to the experimental values, demonstrating the validity of the proposed theoretical approach based on apparent critical temperature anisotropy along ab-plane and c-axis, respectively.

6. Conclusions

In conclusion, we presented a theoretical explanation of the resistance peak effect in LTSC and HTSC. The resistance versus temperature curve for layered materials shows a peak when using a four-point contact configuration with the current (and voltage leads, respectively) parallel to the layered structure. The reason of the peak appearance is an apparent critical temperature anisotropy parallel and perpendicular to the layers. More exactly, T_c along c-axis (perpendicular to layers) is higher than T_c along a-axis (parallel to the layers). The apparent T_c anisotropy can have different causes: critical current anisotropy, coherence lengths anisotropy, or interplay between Kosterlitz-Thouless temperature and Josephson coupling energy. The experiments performed of LSCO thin films confirm the validity of the assumption that the observed T_c along CuO planes is lower than T_c across the layers.

This work was supported by CREST (Core Research for Evolutional Science and Technology) of Japan Science and Technology Corporation (JST) and JSPS (Japan Society for the Promotion of Science).

References

[1] Y. Tajima, K. Yamaya, J. Phys. Soc. Jpn. **53**, 495 (1984); **53**, 3307 (1984); Y. Tajima, et al., J. Phys. Soc. Jpn. **55**, 2121 (1986).
[2] H. Yamamoto, et al., Jpn. J. Appl. Phys. **24**, L314 (1984).
[3] R. Akihama, Y. Okamoto, Solid State Comm. **53**, 655 (1985).
[4] A. Nordström, Ö. Rapp, Phys. Rev. B **45**, 12577 (1992); P. Lindqvist, et al., Phys. Rev. Lett. **64**, 2941 (1990).
[5] R. Vaglio, et al., Phys. Rev. B **47**, 15302 (1993).
[6] Y. K. Kwong, et al., Phys. Rev. B **44**, 462 (1991); P. Santhanam, et al., Phys. Rev. Lett. **66**, 2254 (1991); M. Park, et al., Phys. Lett. **75**, 3740 (1995); Phys. Rev. B **55**, 9067 (1997); C. Strunk, et al., Phys. Rev. B **57**, 10854 (1998); B. Burk, et al., J. Appl. Phys. **83**, 1549 (1998); K. Yu. Arutyunov, et al., Phys. Rev. B **59**, 6487 (1999).
[7] L. Fabrega, et al., Physica C **185-189**, 1913 (1991); M. A. Crusellas, et al., Phys. Rev. B **46**, 14089 (1992); M. Suzuki, Phys. Rev. B **50**, 6360 (1994); H. Myoren, et al., Jpn. J. Appl. Phys. **36**, 2642 (1997).
[8] C. Buzea, Electronic properties due to anisotropy in high-temperature superconductors, Ph. D. Thesis, Tohoku University, Sendai, Japan, (2000); C. Buzea, et al., Adv. Cryogenics Eng. **46**, 607 (1999); C. Buzea, et al., Adv. Cryogenics Eng. **46**, 615 (1999).
[9] Z. He, et al., Solid State Comm.**76**, 671 (1990); J. Mosquiera, et al., J. Appl. Phys. **76**, 1943 (1994); J. Mosquiera, et al., Physica C **225**, 34 (1994); A. C. Bodi, Solid State Comm. **90**, 369 (1994); I. Kirschner, et al., Physica C **252**, 22 (1995).
[10] Y. Zhao, et al., Phys. Rev. B **51**, 3134 (1995); S. H. Han, et al., Solid State Comm. **101**, 899 (1997); F. Hamed, et al., Physica C **293**, 277 (1997).
[11] N. Ihara, T. Matsushita, Physica C **257**, 223 (1996); C. P. poole, H. A. Farach, R. J. Creswick, Superconductivity (Academic Press, San Diego, 1995).
[12] M. Tinkham, Introduction to superconductivity (McGraw Hill, Singapore, 1996).
[13] C. P. Poole, Jr., et al., Characteristic Parameters, in Handbook of Superconductivity, Ed. C. P. Poole, Jr., academic Press, San Diego, 2000, pp. 433-491.
[14] M. Suzuki, Phys. Rev. B **50**, 6360 (1994).
[15] C. Buzea at al., J. Appl. Phys. **86**, 2856 (1999).